INTERNATIONAL JOURNAL OF ROBUST AND NONLINEAR CONTROL
Int. J. Robust Nonlinear Control (2017)
Published online in Wiley Online Library (wileyonlinelibrary.com). DOI: 10.1002/rnc.3784

Robust consensus of unicycles using ternary and hybrid controllers

Matin Jafarian*,†

Department of Automatic Control, School of Electrical Engineering, KTH Royal Institute of Technology, Osquldas väg 10, 10044, Stockholm, Sweden

SUMMARY

This paper presents consensus of the orientations and average positions for a group of unicycles using ternary and hybrid controllers. The decentralized controllers designed to reach consensus of the average positions take only values in the set $\{-1, 0, +1\}$. In addition, a hybrid controller is introduced to control the orientations. Finite-time practical consensus of the average positions is proven despite the simple ternary control laws together with asymptotic consensus of the orientations. Furthermore, the consensus problem is studied in the presence of matched input disturbances that are locally rejected using an internal-model-based controller. The analysis is performed in a hybrid framework. Simulation results illustrate the effectiveness of the design. Copyright © 2017 John Wiley & Sons, Ltd.

Received 20 March 2015; Accepted 25 January 2017

KEY WORDS: consensus; nonholonomic systems; discontinuous dynamical systems; hybrid dynamical systems; internal-model-based approach

1. INTRODUCTION

Distributed motion coordination of mobile agents has attracted increasing attention in the recent years owing to its wide range of applications from biology and social networks to sensor/robotic networks. Consensus (agreement) problem is a well-studied motion coordination problem (e.g., [1–5]) where the goal is to reach a common value for variables of interests, for example, position and orientation.

This paper studies a consensus problem considering three main areas: ternary and hybrid controllers, nonholonomic unicycles, and disturbance rejection. The term nonholonomic refers to motion constraints that depend on both configurations and velocities. Stabilizing both the position and heading of this type of system is challenging, because it does not satisfy the Brockett's necessary condition for stabilization using smooth feedback [6]. The latter has motivated the design of time-varying, nonsmooth, and hybrid controllers in coordination of these dynamic agents ([4, 7–11] to name a few). Smooth time-varying control laws for a network of unicycles have been designed to study the feasibility of stabilizing the network over a directed graph [8], consensus of the speeds and headings [10], and consensus of only the positions of unicycles [11]. Examples of hybrid controllers for unicycles include steering a single unicycle subject to input constraints and through obstacles [12] and deployment of a group of unicycles using locational optimization [13].

Considering nonsmooth controllers, a time-invariant discontinuous controller has been designed in [7] for consensus of unicycles over static and switching topologies. The interest behind designing nonsmooth controllers is not limited to specific dynamical properties, for example, nonholonomic property, of a system. In fact, the real-world constraints, that is, communication and information constrains, in implementation of coordination algorithms have motivated the use of a specific class

*Correspondence to: Matin Jafarian, Department of Automatic Control, School of Electrical Engineering, KTH Royal Institute of Technology, Osquldas väg 10, 10044, Stockholm, Sweden.
†E-mail: matinj@kth.se

of nonsmooth controllers that are based on quantized and coarse information, for example, binary and ternary controllers. For instance, papers [14–17] have studied binary information and control in consensus and formation-keeping problems for a group of continuous-time dynamical systems including single/double integrators and strictly passive systems. A rendezvous problem for Dubins cars based on a ternary feedback has been studied in [18].

Another of main challenges in coordination problems is to reach and maintain the desired goals despite input disturbances (robustness of the design). In this regard, different approaches have been pursued in the literature to deal with disturbances for some classes of dynamical systems. In particular, the role of internal model principle [19] has been studied in coordination problems in order to reject input disturbances of incrementally passive systems [20] and strictly passive systems with binary controllers [17]. An internal model-based design has been used to reject matched input disturbances for a group of wheeled robots controlled by smooth controllers in a port-Hamiltonian framework [21].

Main contribution. This paper considers consensus of continuous-time nonholonomic unicycles assuming that they have a common sense of direction, for example, they are equipped with compass sensors. Compared with the current literature, the contribution of this paper is as follows:

(i) We use only ternary controllers to achieve finite-time practical consensus of the average positions. Our design, which is motivated by real-world constraints in coordination problems, is based on simple control commands. Recent literature in this line of research (e.g., [15–17]) has mainly introduced binary controllers for the position coordination of other classes of dynamic agents and shown exact convergence to the desired formations. This paper uses ternary controllers for unicycles. The application of ternary controllers results in a practical convergence. Despite our coarse control law, the control action shows a steady chatter-free behavior.

(ii) We introduce a hybrid design to control the orientations of the unicycles. We refer to this controller as a *hybrid-quantizer-based* controller because the hybrid design is used to treat the discontinuities of a planar quantizer that is derived based on an application of the atan2 function. The latter is a discontinuous 4-quadrant arctan function. In comparison with the literature (in specific with [7]), one of our major contributions is to consider the discontinuity of the atan2 function in our design. Moreover, the atan2 function has been used in [7] for controlling the orientations of unicycles based on their continuous positions; however, we consider an application of the atan2 function based on the quantized average positions. The latter leads to the design of hybrid-quantizer-based controllers that render the dynamics of the whole system hybrid. In comparison with [22], where a hybrid design has been introduced based on uniform quantizers for the consensus of the positions of single integrators, we present a different hybrid quantizer. The differences of our design include the jump mechanism (discrete transitions) and the design of flow and jump sets.

(iii) For the network of unicycles with the ternary controllers, we study the disturbance rejection problem in a hybrid framework and prove an asymptotic consensus despite the presence of the matched input disturbances.

A partial and preliminary version of this paper without the results of disturbance rejection has been presented in [23].

The outline of this paper is as follows. First, we recall some preliminaries on graph theory, hybrid time-domain framework, and analytical tools for nonsmooth systems. Section 2 presents the motivation and problem formulation. Section 3 introduces the control design and hybrid model of the system. Section 4 presents the closed-loop analysis of the network. Section 5 continues with the analysis in the presence of the matched input disturbances. Section 6 illustrates the simulation results. Finally, Section 7 concludes the paper.

Notations

The symbol $\times_{k=1}^{m} A_k$ denotes the Cartesian product $A_1 \times A_2 \times \ldots \times A_m$. The symbol $\varnothing$ denotes the empty set. Given two matrices A and B, the symbol $A \otimes B$ denotes the Kronecker product. For

DOI: 10.1002/rnc

a function f, dom denotes its domain, and the notation $f^{-1}(r)$ stands for the $r-$level set of f on dom f, that is, $f^{-1}(r) := \{z \in \text{dom } f \mid f(z) = r\}$. Finally, S^1 is the unit circle and $a \cdot b$ denotes the inner product of two vectors $a, b \in \mathbb{R}^n$.

1.1. Preliminaries

Graph theory

A graph G is an ordered set $G(\mathcal{V}, \mathcal{E})$ with node-set $\mathcal{V}$ and edge-set $\mathcal{E}$. We consider a network of n agents evolving in $\mathbb{R}^2$. The way in which the agents exchange information is modeled by a connected undirected graph. In order to use the tools from graph theory, we assign an orientation to each edge. The orientation can be imposed in an arbitrary manner, and it does not have any effect on the final results. The incidence matrix B associated to $G(\mathcal{V}, \mathcal{E})$ describes which nodes are coupled by an edge. The element $b_{i\ell}$ of B is equal to 1 if node i is the head vertex of edge ℓ, -1 if node i is the tail vertex of edge ℓ, and 0 if there is no edge between i and j. For a graph G with the incidence matrix B, the Laplacian matrix is $L = BB^T$. We define the relative position z_ℓ between agent i and j as follows:

$$z_\ell = \begin{cases} q_i - q_j & \text{if node } i \text{ is the head vertex of edge } \ell \\ q_j - q_i & \text{if node } j \text{ is the head vertex of edge } \ell, \end{cases}$$

where $q_i = (x_i, y_i)^T \in \mathbb{R}^2$ is the position of agent i. By definition of B, we can represent the relative position variable z, with $z \triangleq (z_1^T, \ldots, z_m^T)^T$, $z \in \mathbb{R}^{2m}$, as

$$z = (B^T \otimes I_2)q, \tag{1}$$

which implies that z belongs to the range space $\mathcal{R}(B^T \otimes I_2)$.

Nonsmooth analysis

The definition of Krasovskii set-valued map [24] is now recalled. Consider the system $\dot{x} = f(x)$ where $f(x)$ is a discontinuous function. A Krasovskii set-valued map is defined as follows:

$$\mathcal{K}(f(x)) := \bigcap_{\delta > 0} \overline{\text{co}}(f(B(x, \delta))).$$

The operator $\overline{\text{co}}$ denotes the closed convex hull of a set, and $B(x, \delta)$ denotes a ball centered at x with radius δ.

Denote the set-valued map $\mathcal{K}(f(x))$ by $F(x)$. Let V be a locally Lipschitz continuous function. We define the set-valued derivative of V at x with respect to $\dot{x} \in F(x(t))$ as the set $\dot{\tilde{V}}(x) = \{a \in \mathbb{R} : \exists v \in F(x) \text{ s.t. } a = p \cdot v, \ \forall p \in \partial V(x)\}$, where $\partial V(x)$ denotes the Clarke generalized gradient of V at x. In the case V is differentiable at x, one has $\dot{\tilde{V}}(x) = \{\nabla V \cdot v, \ v \in F(x)\}$.

Hybrid time domain

We recall preliminaries on hybrid dynamical systems [25]. A hybrid time domain is a subset of $\mathbb{R}_{\geq 0} \times \mathbb{N}$ that is the union of infinitely many intervals of the form $[t_j, t_{j+1}] \times j$, where $0 = t_0 \leq t_1 \leq t_2 \ldots$, or of finitely many such intervals with the last one possibly of the form $[t_j, t_{j+1}] \times j$, $[t_j, t_{j+1}) \times j$, or $[t_j, +\infty) \times j$. A hybrid system $\mathcal{H} := (C, F, D, G)$ is defined as

$$\mathcal{H} : \begin{cases} \dot{\zeta} \in F(\zeta) & \zeta \in C \\ \zeta^+ \in G(\zeta) & \zeta \in D, \end{cases} \tag{2}$$

where C is the flow set, D the jump set, F the flow map, and G the jump map. We refer the interested reader to [25] for the formal definition of solutions to the hybrid system (2). The solution $\zeta(t, j)$ is

(i) nontrivial if dom $\zeta(t, j)$ contains at least two points,
(ii) complete if dom $\zeta(t, j)$ is unbounded, and
(iii) precompact if it is both complete and bounded.

DOI: 10.1002/rnc

In this paper, we use a hybrid invariance principle (invariance principle using u_C and u_D functions [25]) to study the convergent behavior of our hybrid system. Note that to use this invariance principle, the hybrid system should be nominally well-posed [25]. We now recall the 'basic assumptions' that are the sufficient conditions for a hybrid system to be nominally well-posed. For hybrid system $\mathcal{H}$ with data (F, G, C, and D), the basic assumptions are

(A1) C and D are closed subsets of $\mathbb{R}^n$.
(A2) $F : \mathbb{R}^n \rightrightarrows \mathbb{R}^n$ is outer semicontinuous and locally bounded relative to C, $C \subset \mathrm{dom}F$, and $F(x)$ is convex $\forall x \in C$.
(A3) $G : \mathbb{R}^n \rightrightarrows \mathbb{R}^n$ is outer semicontinuous and locally bounded relative to D and $D \subset \mathrm{dom}G$.
We now recall a property of an outer semicontinuous set-valued map and the hybrid invariance principle with u_C and u_D functions [25].

Property 1
A set-valued mapping $F : \mathbb{R}^n \rightrightarrows \mathbb{R}^n$ is outer semicontinuous if and only if its graph $\{(x, y) : x \in \mathbb{R}^n, y \in F(x)\} \subset \mathbb{R}^{2n}$ is closed ([25]).

*Theorem 1 (**Corollary 8.4.,** [25])*
Consider a continuous function $V : \mathbb{R}^n \to \mathbb{R}$, continuously differentiable on a neighborhood of C. Suppose that for a given set $U \subset \mathbb{R}^n$,

$$u_C(z) \leq 0, \quad u_D(z) \leq 0 \quad \forall z \in U.$$

Let a precompact solution $\varphi^* \in \mathcal{S}_{\mathcal{H}}$ (where $\mathcal{S}_{\mathcal{H}}$ denotes the set of solutions to $\mathcal{H}$) be such that $\overline{\mathrm{rge}\,\varphi^*} \subset U$. Then, for some $r \in V(U)$, φ^* approaches the nonempty set that is the largest weakly invariant subset of

$$V^{-1}(r) \cap U \cap [\overline{u_c^{-1}(0)} \cup (u_D^{-1}(0) \cap G(u_D^{-1}(0)))]. \tag{3}$$

2. MOTIVATION AND PROBLEM FORMULATION

Consider a network of n unicycles in $\mathbb{R}^2$. Figure 1 shows the configuration of one of the agents in $\mathbb{R}^2$. The kinematic model of each of the agents follows

$$\begin{aligned} \dot{x}_i &= u_i \cos\theta_i \\ \dot{y}_i &= u_i \sin\theta_i \\ \dot{\theta}_i &= \omega_i, \end{aligned} \tag{4}$$

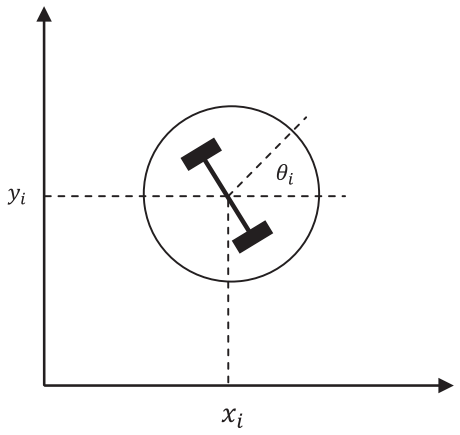

Figure 1. Configuration of a unicycle in $\mathbb{R}^2$.

DOI: 10.1002/rnc

where x_i and y_i are the positions of agent i and θ_i is the orientation of the heading of unicycle i with respect to the x-axis. We consider n unicycles in $\mathbb{R}^2$ communicating over a connected and undirected graph. Let N_i denote the set of neighboring agents of agent i and define the local average position for agent i in x and y directions as $\sum_{j\in N_i}(x_i - x_j)$ and $\sum_{j\in N_i}(y_i - y_j)$. Considering the definition of the Laplacian L, we define the local average positions as follows:

$$L_i x = \sum_{j\in N_i}(x_i - x_j), L_i y = \sum_{j\in N_i}(y_i - y_j),$$

such that $Lx = (L_1 x, \ldots, L_n x)$ and $Ly = (L_1 y, \ldots, L_n y)$. Our goal is to reach a configuration for the agents of the network such that the norms of the local average position of each agent in x and y directions remain in a desired neighborhood of zero. Moreover, we aim at achieving identical orientations for all of the agents. In particular, for each agent i, $L_i x$ and $L_i y$ converge to a desired δ neighborhood of zero while θ_i converges to zero. In detail, the desired goals are

(i) $|L_i x| \leq \delta$ and $|L_i y| \leq \delta$, and
(ii) $\theta_i = 0$,

where $\delta > 0$ is a design choice.

It is well known that the unicycle in (4) is subject to a nonholonomic constraint given by $\dot{x}_i \sin\theta_i - \dot{y}_i \cos\theta_i = 0$. According to Brockett's condition [6], this constrain prevents the state of the system in (4) to be stabilized by means of a smooth controller. The latter has been the motivation behind designing nonsmooth controllers in the literature. The model in (4) can be seen as a nonlinear single integrator. The known control design for consensus of a network of single integrators [1] with the dynamics $\dot{x}_i = u_i$, $\dot{y}_i = v_i$ is $u_i = -L_i x$, $v_i = -L_i y$. Now, consider (4) where $\dot{x}_i \cos\theta_i + \dot{y}_i \sin\theta_i = u_i$ holds. The latter equality motivate us to design a nonsmooth controller as a function of $L_i x \cos\theta_i + L_i y \sin\theta_i$. In this regard, [7] proposed a nonsmooth controller to reach asymptotic consensus of the positions of the agents. Comparing with [7], our proposed position controller only takes values in the set $\{-1, 0, 1\}$. Moreover, we introduce a different design to control the orientations. Our design achieves consensus of the orientations by means of hybrid controllers that are robust to perturbations (Remark 1). The introduction of hybrid-quantizer-based design requires presenting the network model and analysis in the hybrid framework. In the next section, we present the model, control design, and analysis using the tools from hybrid time-domain framework [25].

3. MODEL AND DESIGN

In this section, we present the control design and the closed-loop dynamics. For each nonholonomic agent with the dynamics given in (4), design

$$\begin{aligned} u_i &= -\text{sign}_\varepsilon(L_i x \cos\theta_i + L_i y \sin\theta_i) \\ \omega_i &= -(\theta_i - \theta_i^*), \end{aligned} \tag{5}$$

where the function $\text{sign}_\varepsilon : \mathbb{R} \to \{-1, 0, +1\}$ is defined as follows:

$$\text{sign}_\varepsilon(q) = \begin{cases} +1 & q > \varepsilon \\ -1 & q < -\varepsilon \\ 0 & |q| \leq \varepsilon. \end{cases}$$

Also, in (5), $L_i x$ and $L_i y$ are the local average positions of agent i in x and y directions, respectively. As it can be inferred by the definition of sign_ε function, the controller u_i only takes values $+1$, -1, or 0. The reference signal θ_i^* in (5) will be designed in the next section and depends on the local average position of agent i. It is assumed that all of the agents have a common sense of direction. For instance, each robot is equipped with a navigation sensor such as a compass. A hybrid-quantizer-based controller is introduced to determine θ_i^*. The latter controller renders the dynamics of each of the agents hybrid. Before presenting the design and for the sake of brevity, we define $\ell_i = (L_i x, L_i y)^T$ and $r_i = L_i x \cos\theta_i + L_i y \sin\theta_i$.

DOI: 10.1002/rnc

3.1. Hybrid model

Define the state of each agent by $\zeta_i = (x_i, y_i, \theta_i, \alpha_i, \beta_i)$ with $(x_i, y_i, \theta_i) \in \mathbb{R} \times \mathbb{R} \times S^1$ and (α_i, β_i) is a vector in $\mathbb{R}^2$. In order to present the hybrid model of each of the agents, we first define the flow and jump sets and their corresponding maps. Define $\mathcal{Z}_i = \mathbb{R} \times \mathbb{R} \times S^1 \times \{(0,-1),(1,1)\}$ and

$$\begin{aligned} \bar{C}_i &= \{\zeta_i \in \mathcal{Z}_i : \beta_i(\max(|L_i x|, |L_i y|)) \geq \alpha_i \gamma + (\alpha_i - 1)\delta\} \\ \bar{D}_i &= \{\zeta_i \in \mathcal{Z}_i : \beta_i(\max(|L_i x|, |L_i y|)) \leq \alpha_i \gamma + (\alpha_i - 1)\delta\}, \end{aligned} \tag{6}$$

where $0 < \varepsilon < \gamma < \delta$. The definition of $\mathcal{Z}_i$ refers to two modes for each agent: $(\alpha_i, \beta_i) = (0,-1)$ and $(\alpha_i, \beta_i) = (1,1)$. The aim of designing these two modes is to steer the reference value for the orientation of each of the unicycles to zero when its position approaches the desired neighborhood (a detailed explanation is given in Section 3.3). Considering these modes (see section 1.4.1 in [25]), we define the flow and jump sets for each agent i as follows:

$$\begin{aligned} C_i &= (\{(0,-1)\} \times \bar{C}_i) \cup (\{(1,1)\} \times \bar{C}_i) \\ D_i &= (\{(0,-1)\} \times \bar{D}_i) \cup (\{(1,1)\} \times \bar{D}_i). \end{aligned} \tag{7}$$

Recall that $\ell_i = (L_i x, L_i y)$ and $r_i = L_i x \cos\theta_i + L_i y \sin\theta_i$. The flow dynamics of each of the agents obeys

$$\begin{cases} \dot{x}_i = -\text{sign}_\varepsilon(r_i)\cos\theta_i \\ \dot{y}_i = -\text{sign}_\varepsilon(r_i)\sin\theta_i \\ \dot{\theta}_i = -(\theta_i - \alpha_i \breve{u}_i(\ell_i)) \\ \dot{\alpha}_i = 0 \\ \dot{\beta}_i = 0, \end{cases} \tag{8}$$

where u_i and θ_i^* in (5) are defined as $-\text{sign}_\varepsilon(r_i)$ and $\alpha_i \breve{u}_i(\ell_i)$, respectively, (with $\breve{u}_i$ to be defined later). In addition, if the state of agent i meets the jump condition, the following update occurs

$$\begin{cases} x_i^+ = x_i \\ y_i^+ = y_i \\ \theta_i^+ = \theta_i \\ \alpha_i^+ = 1 - \alpha_i \\ \beta_i^+ = -\beta_i. \end{cases} \tag{9}$$

Now, we define the function $\breve{u}_i(\ell_i)$ that depends on the average position of agent i such that $\alpha_i \breve{u}_i(\ell_i)$ determines the reference signal for the state θ_i. The map of $\breve{u}_i(\ell_i)$ is defined in (10) and is plotted in Figure 2.

$$\breve{u}_i(\ell_i) = \begin{cases} \frac{\pi}{4} & \text{if } L_i x \geq \varepsilon \ , \ L_i y \geq \varepsilon \\ -\frac{\pi}{4} & \text{if } L_i x \geq \varepsilon \ , \ L_i y \leq -\varepsilon \\ \frac{3\pi}{4} & \text{if } L_i x \leq -\varepsilon \ , \ L_i y \geq \varepsilon \\ -\frac{3\pi}{4} & \text{if } L_i x \leq -\varepsilon \ , \ L_i y \leq -\varepsilon \\ \frac{\pi}{2} & \text{if } |L_i x| < \varepsilon \ , \ L_i y \geq \varepsilon \\ -\frac{\pi}{2} & \text{if } |L_i x| < \varepsilon \ , \ L_i y \leq -\varepsilon \\ \pi & \text{if } L_i x \leq -\varepsilon \ , \ |L_i y| < \varepsilon \\ 0 & \text{if } L_i x \geq \varepsilon \ , \ |L_i y| < \varepsilon \\ 0 & \text{if } |L_i x| < \varepsilon \ , \ |L_i y| < \varepsilon. \end{cases} \tag{10}$$

The goal of controlling the network is that each of the agent's average position converges to a $\delta > \varepsilon$ neighborhood of zero, and its orientation converges to zero (Section 2).

Remark 1

The function $\breve{u}_i$ is designed based on $atan2(\text{sign}_\varepsilon(L_i y), \text{sign}_\varepsilon(L_i x))$. The inverse trigonometric function $atan2(y,x)$ is equivalent to a four-quadrant arctangent function with domain $(-\pi, \pi]$. The function $atan2$ is a discontinuous function that can be defined as $atan2(0,0) = 0$ and

DOI: 10.1002/rnc

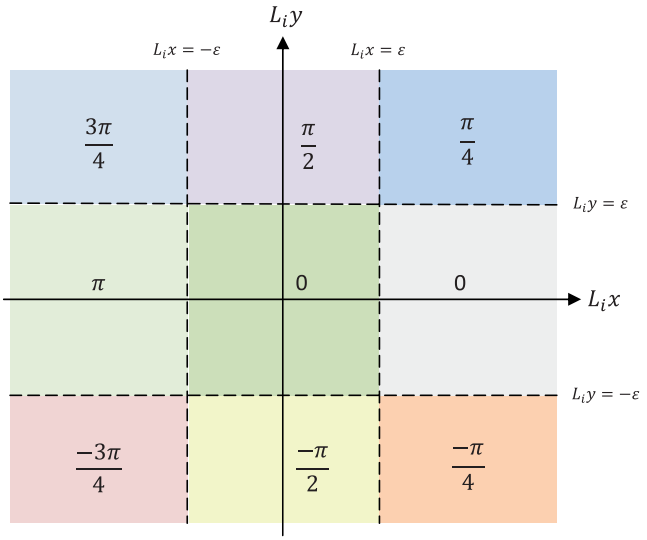

Figure 2. Plot of $\breve{u}_i(\ell_i)$. [Colour figure can be viewed at wileyonlinelibrary.com]

$atan2(y,x) = atan(\frac{y}{x}) + \frac{\pi}{2}\text{sign}(y)(1 - \text{sign}(x))$ [26]. Neglecting the discontinuity of the $atan2$ function will lead in undesired results, that is, the controller will not be robust to the perturbations. As a result, the reference orientation for each agent i, θ_i^* in (5), can take arbitrary values that prevents reaching the consensus on the orientations. The latter is the motivation to introduce a hybrid-based controller.

3.2. (nominally) Well-posed hybrid system

For a system modeled in the hybrid framework of [25], nominally well-posedness is a prerequisite condition that allows using hybrid invariance principles in order to study the asymptotic behavior of the solutions of the hybrid system. Based on [25], the basic assumptions (Section 1.1) are the sufficient conditions for a hybrid system to be nominally well-posed. The basic assumptions imply that C and D should be closed sets and the maps F and G should be locally bounded and outer semicontinuous. Now, we study the nominally well-posedness of the hybrid system defined with the data in (7), (8), and (9).

First, C_i and D_i in (7) are both closed maps. Notice that $C_i \cap D_i \neq \varnothing$. It is worth mentioning that the latter will not harm our analysis if $\delta > \gamma > \varepsilon$ holds. Because, if an agent reaches $C_i \cap D_i$, either it flows or a jump takes place. In case of a jump and considering $\delta > \gamma$, C_i and D_i will be updated such that there will be a hysteresis area between the new C_i and D_i that prevents an immediate consecutive jump (see Section 3.3 for more details). On the other hand, assuming a flow, it can be shown that a jump is eventually inevitable since $\gamma > \varepsilon$ (see the proof of Proposition 3).

Next, Considering the flow dynamics in (8), the right-hand side of the map is discontinuous because of the discontinuity of sign_ε function as well as $\breve{u}_i$ function. In order to meet the required conditions on these maps (see the basic assumptions), we adopt a Krasovskii regularization (see lemma 5.16 in [25]) and define the solutions of the hybrid system in a Krasovskii sense. For this purpose, we define set-valued maps for both flow and jump maps. Moreover, because (8) and (9) are locally bounded, their corresponding set-valued maps are also locally bounded (lemma 5.16 in [25]). Now, we define the corresponding set-valued map for $f_i(\zeta_i)$ in (8) as follows:

$$F_i(\zeta_i) = \begin{pmatrix} \mathcal{K}_1(\text{sign}_\varepsilon(r_i))\cos\theta_i \\ \mathcal{K}_1(\text{sign}_\varepsilon(r_i))\sin\theta_i \\ -(\theta_i - \alpha_i\mathcal{K}_2(\breve{u}_i)) \\ 0 \\ 0 \end{pmatrix}, \tag{11}$$

DOI: 10.1002/rnc

where the set-valued maps $\mathcal{K}_1(.)$ and $\mathcal{K}_2(.)$ are given by

$$\mathcal{K}_1(\text{sign}_\varepsilon(r_i)) = \begin{cases} \{+1\} & \text{if} \quad r_i > \varepsilon \\ \{-1\} & \text{if} \quad r_i < -\varepsilon \\ \{0\} & \text{if} \quad |r_i| < \varepsilon \\ [0,+1] & \text{if} \quad r_i = \varepsilon \\ [-1,0] & \text{if} \quad r_i = -\varepsilon, \end{cases} \tag{12}$$

$$\mathcal{K}_2(\check{u}_i(\ell_i)) = \begin{cases} \{\check{u}_i(\ell_i)\} & \text{if} \ |L_i x| \neq \varepsilon \wedge |L_i y| \neq \varepsilon \\ \bigcap_{\sigma>0} \overline{\text{co}}(\check{u}_i(B(\ell_i,\sigma))) & \text{otherwise,} \end{cases} \tag{13}$$

where $\overline{\text{co}}$ denotes the closed convex hull of a set and $B(\ell_i,\sigma)$ denotes a ball centered at ℓ_i with radius σ. Note that in deriving the set-valued map $\mathcal{K}_1(.)$, we used rules from the calculus of a Krasovskii set valued map (chain rule and equivalent control, rules 4 and 5 in [27]). For instance, because $\cos\theta_i$ ($\sin\theta_i$) is a continuous function, we can write

$$\mathcal{K}_1(\text{sign}_\varepsilon(r_i)\cos\theta_i) = \mathcal{K}_1(\text{sign}_\varepsilon(r_i))\cos\theta_i,$$

and because $r_i = L_i x\cos\theta_i + L_i y\sin\theta_i$ is a continuously differentiable function, we can use the chain rule and define the Krasovskii map for the sign_ε function at $r_i = L_i x\cos\theta_i + L_i y\sin\theta_i$.

In addition, the definition of $\mathcal{K}_2(.)$ implies that on each of the discontinuities, the set-valued map $\mathcal{K}_2(\check{u}_i(\ell_i))$ is equal to a closed interval with lower and upper bounds that are obtained from $\check{u}_i$ function in the vicinity of the discontinuity. For instance, for $L_i x = \varepsilon$ and $L_i y > \varepsilon$, the map $\mathcal{K}_2(\check{u}_i(\ell_i))$ is the closed interval $[\frac{\pi}{4}, \frac{\pi}{2}]$. Or, $L_i x = -\varepsilon$ and $L_i y = \varepsilon$ results in the interval $[0,\pi]$.

Based on the earlier set-valued map, we define the hybrid system $\mathcal{H}$ with the data C, F, D, and G as follows:

$$\begin{aligned} C &= \{\zeta \in \mathcal{Z} : \forall i \in \mathcal{E}, \zeta_i \in C_i\}, \\ D &= \{\zeta \in \mathcal{Z} : \exists i \in \mathcal{E}, \zeta_i \in D_i\} \end{aligned} \tag{14}$$

with $\mathcal{Z} = \mathbb{R}^{2n} \times (S^1)^n \times \{(0,-1),(1,1)\}^n$. If $\zeta \in C$, the system dynamics follows $\dot{\zeta} \in F(\zeta)$, where $F(\zeta) = (F_1^T(\zeta_1), \ldots, F_n^T(\zeta_n))^T$. If $\zeta \in D$, the following discrete update occurs:

$$\begin{aligned} x^+ &= x \\ y^+ &= y \\ \theta^+ &= \theta \\ \alpha_i^+ &= 1 - \alpha_i \\ \beta_i^+ &= -\beta_i. \end{aligned}$$

The dynamic model of the network follows

$$\mathcal{H} : \begin{cases} \dot{\zeta} \in F(\zeta) & \zeta \in C \\ \zeta^+ \in G(\zeta) & \zeta \in D \end{cases} \tag{15}$$

where $G(\zeta) := \{G_i(\zeta_i) : i \in \mathcal{E}\}$ with $G_i(\zeta_i)$, such that agent i meets the jump condition, is given by ([28, 29])

$$G_i(\zeta_i) = (x_1, y_1, \theta_1, (\alpha_1,\beta_1), \ldots, x_i, y_i, \theta_i, (1-\alpha_i, -\beta_i), \ldots, x_n, y_n, \theta_n, (\alpha_n,\beta_n))^T. \tag{16}$$

According to the map in (16), at each jump, the map $G(z)$ updates the state of only one of the agents that meets the jump condition. If more than one agent meet the jump condition simultaneously, only the state of one of them will be updated at the jump. In this case, the system will experience consecutive jumps where the number of jumps is upper bounded by n. The map $G(z)$ is the union of n closed maps G_i given in (16). Hence, $G(z)$ is outer semicontinuous.

DOI: 10.1002/rnc

3.3. *Interpretation of the design*

In this section, we motivate the design of the hybrid-quantizer-based controller and the choices of ε, δ, and γ. Consider (5) and assume that $\theta_i^* = \check{u}_i(\ell_i)$. Recall the plot in Figure 2 and assume that for agent i, the size of average positions in both x and y directions take values equal or smaller than a desired ε. Therefore, based on the map in (10) (also Figure 2), $\check{u}_i(\ell_i)$ should take a zero value. However, if $|L_i x|$, $|L_i y|$ or both of them equal to ε, one cannot guarantee that the unique value for $\check{u}_i$ will remain zero in case of small perturbations, because the map $\check{u}_i(\ell_i)$ is discontinuous at $|L_i x| = \varepsilon$ and $|L_i y| = \varepsilon$. The latter is the motivation behind designing a hybrid map for θ_i^* and choosing $\gamma > \varepsilon$ that adds a hysteresis area to the discontinuous function $\check{u}_i(\ell_i)$ and prevents the undesired values in the vicinity of the discontinuities.

Here, we elaborate on the design by means of an example. Before presenting the example, we remind that the motivation behind $\gamma > \varepsilon$ is to jump over the discontinuities (to prevent the undesired values for the reference signal of the orientation), and the motivation behind $\delta > \gamma$ is to prevent

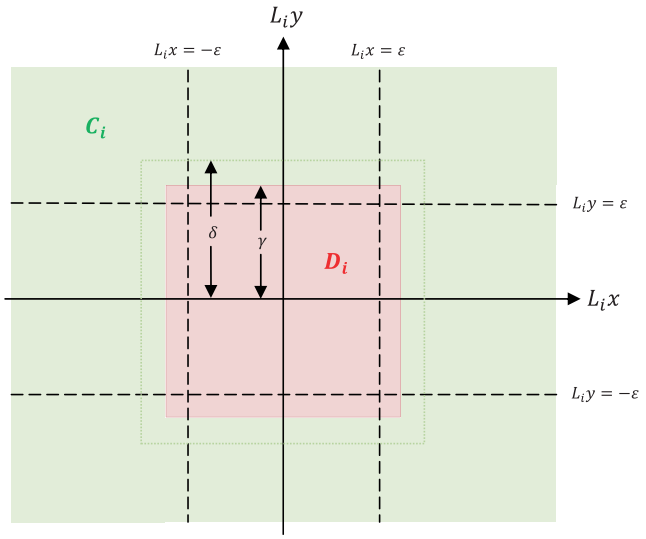

Figure 3. The plot of C_i and D_i at $(t, 0)$. [Colour figure can be viewed at wileyonlinelibrary.com]

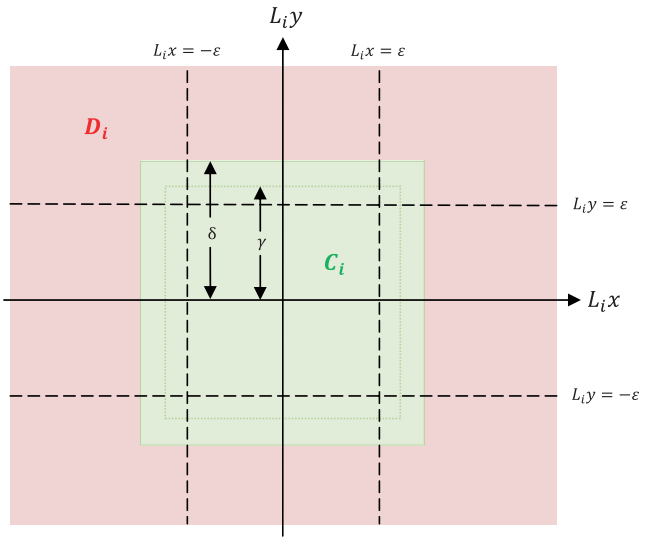

Figure 4. The plot of C_i and D_i at $(t, 1)$. [Colour figure can be viewed at wileyonlinelibrary.com]

DOI: 10.1002/rnc

consecutive jumps between C_i and D_i. Now, we are ready to present the example. Assume that each of the agents initially starts from C_i. Consider $(\alpha_i(t_0), \beta_i(t_0)) = (1, 1)$. The dynamic of agent i starts to evolve based on the set-valued map $F_i(\zeta_i)$ until the condition $\max(|L_i x|, |L_i y|) \geq \gamma$ is violated. At this time, the state of the system will be updated according to the jump map $G_i(\zeta_i)$. Based on the map $G_i(\zeta_i)$ in (9), the states x_i, y_i, and θ_i will stay unchanged, yet α_i and β_i will be updated to 0 and -1 accordingly. Hence, at the jump, the jump and flow sets switch such that the system continues to flow with the only difference being in the reference signal for the state θ_i. Figures 3 and 4 show the flow and jump sets at hybrid times $(t, 0)$ and $(t, 1)$, respectively. Note that the assumption that each of agents initially starts from C_i is made to elaborate on the example and it is not required for the analysis.

4. MAIN RESULTS AND ANALYSIS

In this section, we present the analysis of the network modeled in (15). First, the properties of the solutions are presented. Next, we prove a convergence of the local average positions in finite-time together with the asymptotic convergence of the orientations.

4.1. Basic properties of the solutions

Before presenting the analysis of the system, we discuss the basic properties (existence and completeness) of maximal solutions to the system. Moreover, we show that the solutions of the system undergo a locally finite number of switchings that implies the solutions do not exploit finite accumulations of switching times.

Lemma 1
Every maximal solution $\zeta(t, j)$ to (15) is complete.

Proof
First, we show that for each $\zeta(0, 0)$, there exists a nontrivial solution $\zeta(t, j)$ to (15). For every initial condition, if $\zeta(0, 0) \in C$, the solution to $\dot{\zeta} \in F(\zeta)$ exists because the right-hand side of the differential inclusion

$$\begin{pmatrix} \dot{x}_i \\ \dot{y}_i \end{pmatrix} \in \begin{pmatrix} \mathcal{K}_1(\text{sign}_\varepsilon(r_i)) \cos\theta_i \\ \mathcal{K}_1(\text{sign}_\varepsilon(r_i)) \sin\theta_i \end{pmatrix}$$

is bounded [24]. Also, depending on α_i, we have either $\dot{\theta}_i \in -(\theta_i - \mathcal{K}_2(\check{u}_i(\ell_i)))$ or $\dot{\theta}_i = -\theta_i$. Note that $\mathcal{K}_2(\check{u}_i(\ell_i))$ is measurable and locally bounded. Hence, in both cases, boundedness of the right-hand side of the system's differential inclusion implies existence of the solutions. Alternatively, if $\zeta(0, 0) \in D$, then $\zeta(0, j) \in C$, and the discrete transition stops in j steps such that $1 \leq j \leq n$. We argue as follows. If $\zeta(0, 0) \in D$, there exists at least one (at most n) agent (agents) such that $\zeta_i(0, 0) \in D_i$. The latter implies an update of the state of agent i. According to the update map, D_i and C_i switches, and the variables α_i and β_i will be updated. But now, $\zeta_i(0, 1) \in C_i$. If there are $j \geq 0$ agents with $\zeta_i(0, 0) \in D_i$, after j jumps, we obtain $\zeta(0, j) \in C$. Notice that because $\delta > \gamma$, after the jumps $C \cap D = \varnothing$. Thereafter, one can discuss the existence of the solutions based on a similar argument as for the case $\zeta(0, 0) \in C$. Hence, the solution $\zeta(t, 0)$ starting either from $\zeta(0, 0) \in C$ (or the solution $\zeta(t, j)$ starting from $\zeta(0, j)$ with $\zeta(0, 0) \in D$) exists for t sufficiently close to zero.

Consider maximal solutions. Let us show that such a solution is complete. By contradiction, $dom\zeta$ is bounded, that is, $dom\zeta$ is the union of finitely many intervals of the form $[t_j, t_{j+1}] \times j$, with the last interval either of the form $[t_j, t_{j+1}] \times j$ or $[t_j, t_{j+1}) \times j$ and $t_{j+1} < +\infty$. This yields a contradiction, because in view of the form of the last interval, no more discrete transitions take place and as we showed earlier by $\dot{\zeta} \in F(\zeta)$, the continuous evolution exists for t sufficiently close to zero. □

Lemma 2
For every initial condition $\zeta(0, 0)$, the set of switching times of the solution $\zeta(t, j)$ is locally finite.

DOI: 10.1002/rnc

Proof
For each agent i, a switching occurs when the average position of its neighbors crosses either γ or δ limits. Consider agent i. Depending on α_i and β_i, assume that its related $L_i x$ and $L_i y$ are greater than γ or smaller than δ. Now, a jump will occur for agent i if one of $L_i x$ or $L_i y$ (or both of them) hits the γ (or δ) limit. Because the maximum of the norm of velocity of each agent in both x and y directions is bounded by one, then $L_i \dot{x}$ and $L_i \dot{y}$ are upper bounded by $2N_i$, where N_i is the number of neighboring agents of agent i. Hence, there will be a nonzero minimum time interval between each two consecutive jumps for agent i. This implies a lower bound on the inter-switching time for each agent and ends the proof. □

Auxiliary system: Before presenting the analysis, we write the system's dynamics in terms of the relative positions. Define the position vector $q = (q_1, \ldots, q_n)$, where $q_i = (x_i, y_i)$. Consider the relative position vector z that is defined as $z = (B^T \otimes I_2)q$ with $z = (z_1, \ldots, z_m)$, where $z_k = (z_{k,x}, z_{k,y})$, $z_{k,x} = x_i - x_j$ and $z_{k,y} = y_i - y_j$. Define $\chi = (z, \theta, \alpha, \beta)$ and the hybrid system $\mathcal{H}^z$ with the data C, F^z, D, and G^z as follows:

$$\mathcal{H}^z : \begin{cases} \dot{\chi} \in F^z(\chi) & \chi \in C \\ \chi^+ \in G^z(\chi) & \chi \in D \end{cases} \tag{17}$$

where C and D are defined as in (14) and $F^z(\chi)$ is defined later in (18). Because $z = (B^T \otimes I_2)q$, we have $\dot{z} = (B^T \otimes I_2)\dot{q}$, where $\dot{q} = (\dot{x}, \dot{y})$ with $\dot{x}_i$, $\dot{y}_i$ defined in (11) and (8). Hence, the map $F^z(\chi)$ obeys

$$F^z(\chi) = \begin{pmatrix} F^a(z) \\ F^b(\theta) \\ \mathbf{0} \\ \mathbf{0} \end{pmatrix}, \tag{18}$$

where $\dot{\theta} = (\dot{\theta}_1, \ldots, \dot{\theta}_n)$, $\dot{\theta} \in F^b(\theta)$ with $\dot{\theta}_i \in -(\theta_i - \alpha_i \mathcal{K}_2(\breve{u}_i(\ell_i)))$ and ((12) and (13))

$$\dot{z} \in F^a(z) = (B^T \otimes I_2) \begin{pmatrix} \mathcal{K}_1(\text{sign}_\varepsilon(r_1)) \cos\theta_1 \\ \mathcal{K}_1(\text{sign}_\varepsilon(r_1)) \sin\theta_1 \\ \vdots \\ \mathcal{K}_1(\text{sign}_\varepsilon(r_n)) \cos\theta_n \\ \mathcal{K}_1(\text{sign}_\varepsilon(r_n)) \sin\theta_n \end{pmatrix}. \tag{19}$$

During each jump, $z^+ = z$ and $\theta^+ = \theta$ hold, and only one of the agents updates its α_i and β_i according to the map in (16). Hence, the map G^z follows a similar definition as in (15) and (16).

Lemma 3
The solutions to system (17) are such that $\theta(t, j)$, $\alpha(t, j)$, and $\beta(t, j)$ are bounded.

Proof
The orientation θ_i obeys a linear dynamics with a bounded input. Recalling from (11), $\dot{\theta}_i$ either equals to $-\theta_i$ or belongs to the set $-\theta_i - \mathcal{K}_2(\breve{u}_i(\ell_i)))$ (depends on α_i). Because $\mathcal{K}_2(\breve{u}_i(\ell_i))) \in S^1$ is bounded and $\theta_i(0, 0) \in S^1$, hence $\theta_i(t, j)$ is bounded. Moreover, α_i and β_i take values in the bounded set $\{(0, -1), (1, 1)\}$ that ends the proof. □

Proposition 1
Any maximal solution to the hybrid system (17) is precompact.

Proof
Take the positive-definite, continuously differentiable, and radially unbounded function $V(z) = \frac{1}{2} z^T z$ as the Lyapunov candidate, where z is the relative position vector. First, we argue that the level sets of $V(z)$ are compact sets. Second, we show that the level sets of $V(z)$ are invariant with respect to z. Hence, we can conclude boundedness of $z(t, j)$ initiated from the level sets of $V(z)$.

DOI: 10.1002/rnc

Consider $\Omega_c = \{z | V(z) \leq \frac{c}{2}\}$ with $c \in \mathbb{R}^+$. Because $V(z) \geq 0$ is a continuous function, its graph is closed. Hence, the set Ω_c is a closed set, that is, Ω_c contains its own boundaries $V(z) = \frac{c}{2}$. Moreover, the set Ω_c is bounded. Notice that at jumps $z^+ = z$. By definition of Ω_c, we have $\frac{1}{2} z^T z \leq \frac{c}{2}$ and consequently $\frac{1}{2}\sum_k ||z_k||^2 \leq \frac{c}{2}$. Hence, $0 \leq ||z_k||^2 \leq c$ and $(x_i - x_j)^2 + (y_i - y_j)^2 \leq c$. The latter implies that $|x_i - x_j| \leq \sqrt{c}$ and $|y_i - y_j| \leq \sqrt{c}$. Therefore, each element of the vector z belongs to the set Ω_c is bounded. We can write

$$\Omega_c = \{z \in \mathbb{R}^{2m} | z = (z_{1,x}, z_{1,y}, \ldots, z_{m,x}, z_{m,y}) \ , \ |z_{k,x}| \leq \sqrt{c}, |z_{k,y}| \leq c \ \text{ for } k \in \mathcal{E}\}. \quad (20)$$

The earlier implies that Ω_c is compact with respect to the relative position. Note that in Ω_c, we have $\sum_k z_{k,x}^2 + z_{k,y}^2 \leq c$ that implies that $|L_i x| \leq \sqrt{c}$ and $|L_i y| \leq \sqrt{c}$. Moreover, in the set Ω_c, we have $|L_i x \cos\theta_i + L_i y \sin\theta_i| \leq \sqrt{c}$ (i.e., $|r_i| \leq \sqrt{c}$) because $|\cos\theta_i| \leq 1$ and $|\cos\theta_i| \leq 1$.

Now, we show that the Lyapunov function $V(z)$ is nonincreasing if the relative position z starts from Ω_c. From (17), for all $\chi \in D$, we have $z^+ = z$. Hence, $V(t, j+1) = V(t, j)$. Because $F^z(\chi)$ is a set-valued map, for $\chi \in C$, we calculate the set-valued derivative $\dot{\tilde{V}} = \{dV \cdot \nu | \nu \in F^a(z)\}$, where $F^a(z)$ is a set-valued map defined in (19). First we write,

$$\begin{aligned} V &= \frac{1}{2} z^T z = \frac{1}{2} q^T (B \otimes I_2)(B^T \otimes I_2) q = \frac{1}{2}(x^T L x + y^T L y) \\ &= \frac{1}{2} \sum_i \sum_{j \in N_i} (x_i - x_j)^2 + (y_i - y_j)^2. \end{aligned}$$

Then,

$$\begin{aligned} \dot{\tilde{V}} &= \left\{ \frac{1}{2} \sum_i \sum_{j \in N_i} (2(x_i - x_j), 2(y_i - y_j)) \begin{pmatrix} \dot{x}_i \\ \dot{y}_i \end{pmatrix} \right\} \\ &= \left\{ \sum_i \left(\sum_{j \in N_i} (x_i - x_j) \right), \sum_{j \in N_i} (y_i - y_j)) \begin{pmatrix} \dot{x}_i \\ \dot{y}_i \end{pmatrix} \right\} \\ &= \left\{ \sum_i (L_i x, L_i y) \begin{pmatrix} u_i \cos\theta_i \\ u_i \sin\theta_i \end{pmatrix} \right\}. \end{aligned} \quad (21)$$

Recall from (12) that $u_i = -\mathcal{K}_1(\text{sign}_\varepsilon(r_i))$. Hence, we have

$$\dot{\tilde{V}} = \{dV \cdot \nu | \nu = (\nu_{1,x}, \nu_{1,y}, \ldots, \nu_{n,y}) \ , \ \nu_{i,x} \in \mathcal{K}_1(\text{sign}_\varepsilon(r_i)) \cos\theta_i, \nu_{i,y} \in \mathcal{K}_1(\text{sign}_\varepsilon(r_i)) \sin\theta_i\}.$$

From the definition of the set-valued map in (12), we define $u_i = -\omega^{u_i}$ where $\omega^{u_i} \in \mathcal{K}_1(\text{sign}_\varepsilon(r_i))$. Hence, we obtain

$$\dot{\tilde{V}} = \left\{ -\sum_i r_i \ \omega^{u_i}, \ \omega^{u_i} \in \mathcal{K}_1(\text{sign}_\varepsilon(r_i)), \forall i \in \mathcal{V} \right\}, \quad (22)$$

and $\dot{\tilde{V}} \subseteq (-\infty, 0]$. The latter implies stability of the subsystem $\dot{z} \in (B^T \otimes I_2)\mathcal{K}_1(\dot{q}), z^+ = z$. From this result, together with Lemma 3, we conclude that every maximal solution $\varphi(t, j)$ started from $\Omega_c \times (S^1)^n \times \{(0,-1),(1,1)\}^n$ is bounded. Also, Lemma 1 implies completeness of the maximal solutions to (15) and consequently to (17). Because $\varphi(t, j)$ is both bounded and complete, it is precompact. □

4.2. Convergence results

This section studies the convergence of solutions to the hybrid system (17) using the hybrid invariance principle ('invariance principle using u_C and u_D functions' [25], also see Section 1.1). We prove that the precompact solutions to the system (17) converge to the largest weakly invariant set of

$$\Omega_c \cap [\overline{u_C^{-1}(0)} \cup (u_D^{-1}(0) \cap G(u_D^{-1}(0)))].$$

DOI: 10.1002/rnc

Notice that in the earlier set, $\theta_i \in S^1$ and $(\alpha_i, \beta_i) \in \{(0,-1),(1,1)\}$. Now, for a Lyapunov function $V(z) = \frac{1}{2} z^T z$, we introduce functions u_C and u_D. Define ([25])

$$\begin{aligned} u_D(\chi) &= \begin{cases} \max_{\lambda \in G(\chi)} V(\lambda) - V(z) & \text{if } \chi \in D \\ -\infty & \text{otherwise} \end{cases} \\ u_C(\chi) &= \begin{cases} \max_{v \in F^z(\chi)} \langle \nabla V(z), v \rangle & \text{if } \chi \in C \\ -\infty & \text{otherwise.} \end{cases} \end{aligned} \tag{23}$$

Proposition 2
Any precompact solution to the hybrid system (17) converges in finite-time to the following largest weakly invariant set

$$\{(z, \theta, \alpha, \beta) : |L_i x \cos\theta_i + L_i y \sin\theta_i| \leq \varepsilon, \forall i \in \mathcal{V}\}.$$

Proof
Take the continuously differentiable function $V(z) = \frac{1}{2} z^T z$ as the Lyapunov candidate and consider (23). First, we calculate $u_D(\chi)$. Because V only depends on the continuous variable z and the latter does not undergo any change during jumps, it is immediate to see that $V(\lambda) - V(z) = 0$ for all $\lambda \in G(\chi)$. Therefore, for all $\chi \in D$, $u_D(\chi) = 0$. That is, $V(t, j+1) - V(t, j) = 0$. Hence, $u_D^{-1}(0) = D$. Calculating the set $G(u_D^{-1}(0))$, we obtain the output of the jump map after the first jump. At the first jump, only one of the agents that meets the jump conditions will be updated. Based on the design of the flow and jump maps, the output of the jump map for agent i is the set of points belonging to the flow set C_i. Hence, $G(u_D^{-1}(0))$ contains the points belong to the new flow set C_i. Recall from Remark 1 that after each jump, there will be a hysteresis area between the new C_i and D_i (Figures 3 and 4). Hence, $C_i \cap D_i = \varnothing$. Therefore, we obtain

$$u_D^{-1}(0) \cap G(u_D^{-1}(0)) = \varnothing. \tag{24}$$

To obtain the function $u_C(\chi)$, we calculate $\langle \nabla V(z), v \rangle$, where v belongs to the map F^a in (19). The calculation is similar to (21) and results in (22). In specific, the set $\overline{u_C^{-1}(0)}$, that is, the set on which $0 \in \langle \nabla V(z), v \rangle$ holds, is

$$\Omega_0 = \{(z, \theta, \alpha, \beta) : |L_i x \cos\theta_i + L_i y \sin\theta_i| \leq \varepsilon, \forall i \in \mathcal{V}\}. \tag{25}$$

Now, considering the largest weakly invariant set formulated in (3) together with (24) and (25), we conclude convergence of the precompact solutions to $\mathcal{H}^z$ to the set (25). Note that in Ω_0, $\theta_i \in S^1$ and $(\alpha_i, \beta_i) \in \{(0,-1),(1,1)\}$.

Next, we show that the earlier convergence is reached in finite-time following a similar reasoning in proposition 2.6 of [30]. As explained, the level sets of $V(z)$, $\Omega_c \in \mathbb{R}^{2n}$, are compact and invariant with respect to z and r_i. We show that there must exist a time T such that $\varphi(T, j) \in \Omega_0$. From (22), if $r_i \in \mathbb{R}^2 / \Omega_0$, then $\max \dot{\tilde{V}} < -n\varepsilon < 0$. Now, consider the evolution of $V(z)$ along a solution $\varphi(t, j)$ started in Ω_c. Note that $z^+ = z, \theta^+ = \theta$. Hence, $V(\varphi(t, j+1)) = V(\varphi(t, j))$. We calculate

$$V(\varphi(t, j)) = V(\varphi(0,0)) + \int_0^t \frac{d}{ds} V(\varphi(s, j)) ds < V(\varphi(0,0)) - n\varepsilon t,$$

where for $t \to +\infty$, we conclude $V(\varphi(t, j)) \to -\infty$ that contradicts the boundedness and invariance of Ω_c. Hence, the convergence to Ω_0 is in finite-time that ends the proof. □

Corollary 1
All maximal solutions to the hybrid system (15) are bounded.

Proof
The proof is based on the proof of Proposition 2. As shown, the system (15) converges to the largest weakly invariant set in (25). On this set, either $|r_i| < \varepsilon$ or $|r_i| = \varepsilon$ holds for each agent i. If $|r_i| < \varepsilon$,

DOI: 10.1002/rnc

it immediately follows that $\dot{x}_i = 0$ and $\dot{y}_i = 0$. Now, consider the case where $|r_i| = \varepsilon$. Assume, $r_i = \varepsilon$. Then, according to the Krasovskii map (12), $\dot{x}_i \in [-1, 0]\cos\theta_i$ and $\dot{y}_i \in [-1, 0]\sin\theta_i$. Now, if $\dot{x}_i$ ($\dot{y}_i$) takes a value equal to zero, the x-position (y-position) of agent i will not change and $u_i = 0$. Otherwise, a nonzero value for $\dot{x}_i$ ($\dot{y}_i$) (also depends on the term $\cos\theta_i$ and $\sin\theta_i$) implies that agent i is moving. Because agent i cannot exit the set Ω_0, the motion leads to $|r_i| < \varepsilon$. Hence, $\dot{x}_i$ and $\dot{y}_i$ will eventually become zero. In addition, we have $\dot{x}_i \in [-1, +1]$ and $\dot{y}_i \in [-1, +1]$ because the norm of $\text{sign}_\varepsilon(.)$, $\cos(.)$, and $\sin(.)$ is smaller or equal to one. Hence, provided that the agents start from bounded initial conditions, they evolve with a bounded velocity that eventually goes to zero. Therefore, x_i and y_i are bounded. Moreover, θ_i, α_i, and β_i are also bounded by Lemma 3, then all solution $\zeta(t, j)$ to (15) are bounded. □

Proposition 3
The maximal solutions of the hybrid system (15) converge to the following set

$$\{(x, y, \theta, \alpha, \beta) : \ \forall i \in \mathcal{E} \quad |L_i x| \leq \varepsilon, \ |L_i y| \leq \delta, \ \theta_i = 0, (\alpha_i, \beta_i) = (0, -1) \ \forall i \in \mathcal{V}\}.$$

Proof
Following the proof of Proposition 2 and Corollary 1, we first discuss that on the invariant set Ω_0, $(\alpha_i, \beta_i) = (0, -1)$ should hold for each agent i. In general, the following four possibilities can occur for each agent i:

(i) $(\alpha_i, \beta_i) = (0, -1)$ and $\zeta_i \in D_i$,
(ii) $(\alpha_i, \beta_i) = (1, 1)$ and $\zeta_i \in D_i$,
(iii) $(\alpha_i, \beta_i) = (0, -1)$ and $\zeta_i \in C_i$,
(iv) $(\alpha_i, \beta_i) = (1, 1)$ and $\zeta_i \in C_i$.

If $\zeta_i \in D_i$, after an update, $\zeta_i \in C_i$ holds. Hence, we can brief the earlier four cases to the last two ones. Now, we argue that for each agent i on the set Ω_0, we should have $(\alpha_i, \beta_i) = (0, -1)$ and $\zeta_i \in C_i$. By contradiction, assume that there exists an agent i such that $(\alpha_i, \beta_i) = (1, 1)$. Then by definition of C_i, we will have

$$\max(|L_i x|, |L_i y|) \geq \gamma. \tag{26}$$

Because, on the set Ω_0 the conditions $\dot{x}_i = 0$ and $\dot{y}_i = 0$ hold (based on the proof of Corollary 1), the agents will not change their positions, and therefore, the condition (26) should hold on Ω_0. That means that θ_i will converge to θ_i^*. Now, if $\max(|L_i x|, |L_i y|) \geq \gamma$, θ_i^* will take a value determined by $\mathcal{K}_2(\check{u}_i(\ell_i))$. The latter map can be calculated based on (10) (Figure 2). Here, we provide this map for the case $|L_i x| \geq \gamma$ as follows:

$$\check{u}_i(\ell_i) \in \begin{cases} \{\frac{\pi}{4}\} & \text{if } L_i x \geq \gamma \ , \ L_i y > \varepsilon \\ \{-\frac{\pi}{4}\} & \text{if } L_i x \geq \gamma \ , \ L_i y < -\varepsilon \\ \{\frac{3\pi}{4}\} & \text{if } L_i x \leq -\gamma \ , \ L_i y > \varepsilon \\ \{-\frac{3\pi}{4}\} & \text{if } L_i x \leq -\gamma \ , \ L_i y < -\varepsilon \\ \{\pi\} & \text{if } |L_i x| \leq -\gamma \ , \ |L_i y| < \varepsilon \\ \{0\} & \text{if } |L_i x| \geq \gamma \ , \ |L_i y| < \varepsilon \\ \left[0, \frac{\pi}{4}\right] & \text{if } L_i x \geq \gamma \ , \ L_i y = \varepsilon \\ \left[-\frac{\pi}{4}, 0\right] & \text{if } L_i x \geq \gamma \ , \ L_i y = -\varepsilon \\ \left[\frac{3\pi}{4}, \pi\right] & \text{if } L_i x \leq -\gamma \ , \ L_i y = \varepsilon \\ \left[-\pi, -\frac{3\pi}{4}\right] & \text{if } L_i x \leq -\gamma \ , \ L_i y = -\varepsilon \end{cases} \tag{27}$$

where $\gamma > \varepsilon$. A similar map can be calculated for the case $|L_i x| \geq \gamma$.
Replacing θ_i from the earlier map into the inequality that holds on the invariant set Ω_0 ($|r_i| \leq \varepsilon$) leads to a contradiction. Hence, α_i is necessarily zero for each i, and consequently, $\beta_i = -1$. Note that the earlier argument only proves that on Ω_0, $(\alpha_i, \beta_i) = (0, -1)$ holds and does not infer any result on the size of $L_i x$ and $L_i y$. Next, we discuss that if $\alpha_i = 0$ then $|L_i x| \leq \varepsilon$ and $|L_i y| \leq \delta$. Assuming that α_i is equal to zero on the invariant set Ω_0, we conclude that θ_i will eventually become

DOI: 10.1002/rnc

zero. Hence, because $|r_i| \leq \varepsilon$ should hold, we conclude that $|L_i x| \leq \varepsilon$. Also, because $\alpha_i = 0$, $\max(|L_i x|, |L_i y|) \leq \delta$ holds. Therefore, $|L_i y| \leq \delta$ should necessarily hold that ends the proof. □

Remark 2
It is not necessary for all agents to have the same ε, γ, and δ thresholds. However, for each agent, $\delta_i > \gamma_i > \varepsilon_i$ should hold. Considering the case where agents have different ε_i, γ_i, and δ_i, the consensus of average positions and orientations can still be achieved but the bounds of the consensus region (for the average positions) will depend on the maximum ε_i, δ_i, and the interconnecting topology (Section 6). Calculating this bound is beyond the scope of this paper.

Discussion on the control action u: That control action u_i does not show fast switching behavior after the consensus is achieved (Section 6) despite its coarse nature and in comparison with sign-based controllers (e.g., [17, 31]). The reason can be explained based on the proof of Proposition 2 and Corollary 1. As discussed, on the set Ω_0, the control $u_i = \text{sign}_\varepsilon(r_i)$ is equal to zero if $|r_i| < \varepsilon$. On the other hand, if $|r_i| = \varepsilon$, u_i can take a zero or nonzero value according to the map (12). Consider the latter case. If u_i takes a nonzero value, agent i will move towards the set where $|r_i| < \varepsilon$. Notice that the control of each agent in the x-direction is $u_i \cos\theta_i$ and in the y-direction is $u_i \sin\theta_i$. Because $\sin\theta_i$ and $\cos\theta_i$ cannot be simultaneously equal to zero, then if u_i takes a nonzero value according to the map (12), at least one of the velocities (in x or y directions) will be nonzero. Therefore, agent i will move. However, the control action $u_i(t)$ may show transient fast switching before the consensus is achieved (Section 6).

5. DISTURBANCE REJECTION

This section studies the problem of consensus of nonholonomic unicycles with the consensus controller designed in Section 3 and in the presence of matched input disturbances. We assume that the disturbance affects the position dynamics of each of the agents. For instance, the disturbance occurs at the actuator side of the translational motion. Under this assumption, the dynamics of each agent is

$$\dot{x}_i = (u_i + d_i)\cos\theta_i, \quad \dot{y}_i = (u_i + d_i)\sin\theta_i, \quad \dot{\theta}_i = \omega_i, \tag{28}$$

where d_i is the disturbance. The network should converge to the desired goals (as stated in Section 2) despite the action of disturbance d_i. Moreover, we suppose that the disturbance signal d_i acting on agent i is generated by an exosystem of the form

$$\dot{w}_i^d = \Phi_i^d w_i^d, \quad d_i = \Gamma_i^d w_i^d, \quad i = 1, 2, \ldots, n. \tag{29}$$

To counteract the effect of the disturbances, we introduce an additional internal-model-based controller [19] given by

$$\begin{aligned} \dot{\eta}_i &= \Phi_i^d \eta_i + E_i^d \breve{u}_i \\ \hat{d}_i &= \Gamma_i^d \eta_i, \qquad\qquad i = 1, 2, \ldots, n. \end{aligned} \tag{30}$$

Considering the input disturbance, we can write (28) in the following form:

$$\begin{aligned} \dot{x}_i &= (u_i + d_i - \hat{d}_i)\cos\theta_i \\ \dot{y}_i &= (u_i + d_i - \hat{d}_i)\sin\theta_i, \\ \dot{\theta}_i &= \omega_i. \end{aligned} \tag{31}$$

Define the new variable $\tilde{d}_i = \hat{d}_i - d_i$ and $\tilde{\eta}_i = \eta_i - w_i^d$, then

$$\begin{aligned} \dot{\tilde{\eta}}_i &= \Phi_i^d \tilde{\eta}_i + E_i^d \breve{u}_i \\ \tilde{d}_i &= \Gamma_i^d \tilde{\eta}_i. \end{aligned} \tag{32}$$

DOI: 10.1002/rnc

Designing u_i and ω_i as in Section 3 and considering the new state $\zeta_i = (x_i, y_i, \theta_i, \tilde{\eta}_i, \alpha_i, \beta_i)$, the hybrid model of the network is presented as follows:

$$\begin{aligned} C^d &= \left\{\zeta \in \mathcal{Z}^d : \forall i \in \mathcal{E}, \zeta_i \in (\{(0,-1)\} \times \bar{C}_i^d) \cup (\{(1,1)\} \times \bar{C}_i^d)\right\}, \\ D^d &= \left\{\zeta \in \mathcal{Z}^d : \exists i \in \mathcal{E}, \zeta_i \in (\{(0,-1)\} \times \bar{D}_i^d) \cup (\{(1,1)\} \times \bar{D}_i^d)\right\}, \end{aligned} \tag{33}$$

with $\mathcal{Z}^d = \mathbb{R}^n \times \mathbb{R}^n \times (S^1)^n \times \mathbb{R}^n \times \{(0,-1),(1,1)\}^n$ and

$$\begin{aligned} \bar{C}_i^d &= \left\{\zeta_i \in \mathcal{Z}_i^d : \beta_i(\max(|L_i x|, |L_i y|)) \geq \alpha_i \gamma + (\alpha_i - 1)\delta\right\} \\ \bar{D}_i^d &= \left\{\zeta_i \in \mathcal{Z}_i^d : \beta_i(\max(|L_i x|, |L_i y|)) \leq \alpha_i \gamma + (\alpha_i - 1)\delta\right\}. \end{aligned} \tag{34}$$

The dynamic model of the network follows

$$\mathcal{H}^d : \begin{cases} \dot{\zeta} \in F^d(\zeta) & \zeta \in C^d \\ \zeta^+ \in G^d(\zeta) & \zeta \in D^d. \end{cases} \tag{35}$$

The definition of the jump map G^d is analogous with (16). If $\zeta \in C^d$, the system dynamics is $\dot{\zeta} \in F^d(\zeta)$, where $F^d(\zeta) = ({F_1^d}^T(\zeta_1), \ldots, {F_n^d}^T(\zeta_n))^T$ and

$$F_i^d(\zeta_i) = \begin{pmatrix} -\mathcal{K}_1(\text{sign}_\varepsilon(r_i))\cos\theta_i - \tilde{d}_i \cos\theta_i \\ -\mathcal{K}_1(\text{sign}_\varepsilon(r_i))\sin\theta_i - \tilde{d}_i \sin\theta_i \\ -(\theta_i - \alpha_i \mathcal{K}_2(\breve{u}_i)) \\ \Phi_i^d \tilde{\eta}_i + E_i^d \breve{u}_i \\ 0 \\ 0 \end{pmatrix}. \tag{36}$$

On the other hand, if $\zeta \in D^d$, the following discrete update occurs:

$$x^+ = x, \;\; y^+ = y, \;\; \theta^+ = \theta, \;\; \tilde{\eta}^+ = \tilde{\eta}, \;\; \alpha_i^+ = 1 - \alpha_i, \;\; \beta_i^+ = -\beta_i.$$

To proceed with the analysis and following Section 4, we write the dynamics of the system in terms of the relative positions $z = (B^T \otimes I_2)q$. Define $\chi = (z, \theta, \tilde{\eta}, \alpha, \beta)$ and the hybrid system $\mathcal{H}^{d,z}$ with the data C^d, $F^{d,z}$, D^d, and $G^{d,z}$ as follows:

$$\mathcal{H}^{d,z} : \begin{cases} \dot{\chi} \in F^{d,z}(\chi) & \chi \in C^d \\ \chi^+ \in G^{d,z}(\chi) & \chi \in D^d, \end{cases} \tag{37}$$

where C^d and D^d are defined as in (33) and the map $F^{d,z}(\chi)$ obeys

$$F^{d,z}(\chi) = \begin{pmatrix} F^{d,a}(z) \\ F^{d,b}(\theta) \\ \Phi^d \tilde{\eta} + E^d \breve{u} \\ \mathbf{0} \\ \mathbf{0} \end{pmatrix}. \tag{38}$$

where $F^{d,b}(\theta)$ follows a similar definition as in (18). Because $z = (B^T \otimes I_2)q$, we have $\dot{z} = (B^T \otimes I_2)\dot{q}$. Hence,

$$\dot{z} \in F^{d,a}(z) = (B^T \otimes I_2) \begin{pmatrix} \mathcal{K}_1(\text{sign}_\varepsilon(r_1))\cos\theta_1 - \tilde{d}_1 \cos\theta_i \\ \mathcal{K}_1(\text{sign}_\varepsilon(r_1))\sin\theta_1 - \tilde{d}_1 \sin\theta_i \\ \vdots \\ \mathcal{K}_1(\text{sign}_\varepsilon(r_n))\cos\theta_n - \tilde{d}_n \cos\theta_n \\ \mathcal{K}_1(\text{sign}_\varepsilon(r_n))\sin\theta_n - \tilde{d}_n \sin\theta_n \end{pmatrix}. \tag{39}$$

In this section, we prove that with appropriate choice of E_i^d and $\breve{u}_i$, the internal-model-based controller counteracts the disturbance and the network converges to the desired goals (as stated in

DOI: 10.1002/rnc

Section 2). In what follows, we study the properties of the solutions to $\mathcal{H}^{d,z}$. Next, we present the convergence results using the hybrid invariance principle using u_C and u_D functions in (23) [25]. For the sake of conciseness, some parts of the proofs of this section are briefed because of the similarity with proofs of the previous section.

Let us assume that each agent access the measurement of its own linear velocity. For the closed-loop system in (37), assume $\Phi_i^d = -\Phi_i^{d\,T}$, and design $E_i^d = \Gamma_i^{d\,T}$ and $\breve{u}_i = r_i + \text{sign}_\varepsilon(r_i) + \dot{x}_i \cos\theta_i + \dot{y}_i \sin\theta_i$. Notice that the control law $\breve{u}_i$ is designed to include the terms $\dot{x}_i$ and $\dot{y}_i$ in order to attenuate (reject) the disturbances. The following can be proven.

Proposition 4

Assume that $\Phi_i^d = -\Phi_i^{d\,T}$, $E_i^d = \Gamma_i^{d\,T}$. Design $u_i = -\text{sign}_\varepsilon(r_i)$ and $\breve{u}_i = r_i + \text{sign}_\varepsilon(r_i) + \dot{x}_i \cos\theta_i + \dot{y}_i \sin\theta_i$, where $r_i = L_i x \cos\theta_i + L_i y \sin\theta_i$. Then, all maximal solutions to (37) are precompact and converge to the following largest weakly invariant set

$$\left\{(z, \theta, \tilde{\eta}, \alpha, \beta) : |L_i x \cos\theta_i + L_i y \sin\theta_i| \leq \varepsilon,\ \tilde{d}_i = 0\ \ \forall i \in \mathcal{V}\right\}.$$

Proof

First, we prove the completeness. The proof follows the same line as in the proof of Lemma 1. The only difference is in the flow maps F^z and $F^{d,z}$. But, because the map $F^{d,z}$ is measurable and locally bounded, with the same arguments as in the proof of Lemma 1, we can show existence and completeness of the solutions to (37).

Next, we show that the maximal solutions to the hybrid system (37) are bounded. To this purpose, we follow a similar trend as the proof of Proposition 1. Take $V(z, \tilde{\eta}) = \frac{1}{2} z^T z + \frac{1}{2} \tilde{\eta}^T \tilde{\eta}$ and consider Ω_c^d the compact level sets of $V(z, \tilde{\eta})$. Now, we show that the Lyapunov function $V(z, \tilde{\eta})$ will not increase if the system starts from Ω_c^d. For $\chi \in D^d$, we have $z^+ = z$ and $\tilde{\eta}^+ = \tilde{\eta}$. Hence, for $\chi \in D^d$, $V(t, j+1) = V(t, j)$ holds. Now, consider $\chi \in C^d$. Because $F^{d,z}(\chi)$ is a set-valued map, for $\chi \in C^d$, we calculate the set-valued derivative $\dot{\bar{V}} = \{dV \cdot \nu | \nu \in F^{d,a}(z)\}$. Let us write

$$\begin{aligned} V &= \frac{1}{2} z^T z + \frac{1}{2} \tilde{\eta}^T \tilde{\eta} \\ &= \frac{1}{2} \sum_i \sum_{j \in N_i} (x_i - x_j)^2 + (y_i - y_j)^2 + \frac{1}{2} \sum_i \tilde{\eta_i}^T \tilde{\eta_i}. \end{aligned}$$

Hence,

$$\begin{aligned} \dot{\bar{V}} &= \left\{ \frac{1}{2} \sum_i \sum_{j \in N_i} (2(x_i - x_j), 2(y_i - y_j)) \begin{pmatrix} \dot{x}_i \\ \dot{y}_i \end{pmatrix} + \sum_i \tilde{\eta_i}^T \dot{\tilde{\eta}}_i \right\} \\ &= \left\{ \sum_i (L_i x, L_i y) \begin{pmatrix} u_i \cos\theta_i \\ u_i \sin\theta_i \end{pmatrix} - \sum_i (L_i x \cos\theta_i + L_i y \sin\theta_i) \tilde{d}_i \right. \\ &\quad \left. + \sum_i \tilde{\eta_i}^T \Phi_i^d \tilde{\eta}_i + \sum_i \tilde{\eta_i}^T E_i^d \breve{u}_i \right\}. \end{aligned} \tag{40}$$

Design $E_i^d = \Gamma_i^{d\,T}$. Considering that Φ_i^d is skew-symmetric, (40) simplifies to

$$\dot{\bar{V}} = \left\{ \sum_i (L_i x, L_i y) \begin{pmatrix} u_i \cos\theta_i \\ u_i \sin\theta_i \end{pmatrix} - \sum_i r_i \tilde{d}_i + \sum_i \tilde{\eta_i}^T \Gamma_i^{d\,T} \breve{u}_i \right\}. \tag{41}$$

Now, design $u_i = -\text{sign}_\varepsilon(r_i)$ as in Section 4, and design $\breve{u}_i = r_i + \text{sign}_\varepsilon(r_i) + \dot{x}_i \cos\theta_i + \dot{y}_i \sin\theta_i$. From the definition of the set-valued map in (12), take $u_i = -\omega^{u_i}$, where $\omega^{u_i} \in \mathcal{K}_1(\text{sign}_\varepsilon(r_i))$. Because $\dot{x}_i = (u_i - \tilde{d}_i)\cos\theta_i$ and $\dot{y}_i = (u_i - \tilde{d}_i)\sin\theta_i$, we have

DOI: 10.1002/rnc

$$\begin{aligned}\breve{u}_i &= r_i + \text{sign}_\varepsilon(r_i) + \dot{x}_i \cos\theta_i + \dot{y}_i \sin\theta_i \\ &= r_i + \omega^{u_i} + (-\omega^{u_i} - \tilde{d}_i)\cos^2\theta_i + (-\omega^{u_i} - \tilde{d}_i)\sin^2\theta_i \\ &= r_i - \tilde{d}_i.\end{aligned} \tag{42}$$

Note that $\tilde{\eta}_i^T \Gamma_i^{d\,T} = \tilde{d}_i^T$. Now, considering that $u_i = -\omega^{u_i}$ and $\breve{u}_i = r_i - \tilde{d}_i$, from (41), we obtain the set-valued derivative $\dot{\tilde{V}}$ as follows:

$$\dot{\tilde{V}} = \left\{ -\sum_i r_i\ \omega^{u_i} - \sum_i \tilde{d}_i^T \tilde{d}_i,\ \ \omega^{u_i} \in \mathcal{K}_1(\text{sign}_\varepsilon(r_i)), \forall i \in \mathcal{V} \right\}. \tag{43}$$

Because $\dot{\tilde{V}} \in (-\infty, 0]$, we conclude that $V(z, \tilde{\eta})$ is nonincreasing and $z(t, j)$ and $\tilde{\eta}(t, j)$ are bounded. Because the dynamics of $\dot{\theta}_i$ is not affected by the disturbances, the results of Lemma 3 hold. Hence, from boundedness of $z(t, j)$ and $\tilde{\eta}(t, j)$, together with the results of Lemma 3, we conclude that the maximal solutions to the system (37) are bounded. Hence, they are precompact because both are bounded and complete.

Now, we continue the proof of convergence based on application of the hybrid invariance principle. Following the proof of Proposition 2, we prove that the precompact solutions to the system (37) converge to the largest weakly invariant set of

$$\Omega_c^d \cap [\overline{u_D^{-1}(0)} \cup (u_D^{-1}(0) \cap G(u_D^{-1}(0)))]$$

where the function u_C and u_D are defined in (23) (note that one should consider the data of the hybrid system $\mathcal{H}^{d,z}$, e.g., D^d and C^d). Because the new variable $\tilde{\eta}$ does not affect the definition of the jump and flow sets, we calculate u_D and consequently $u_D^{-1}(0) \cap G(u_D^{-1}(0))$ same as in the proof of Proposition 2. Hence, $u_D^{-1}(0) \cap G(u_D^{-1}(0)) = \varnothing$. Moreover, calculation of u_C leads to the same set as in (43). In specific, $u_C^{-1}(0)$ is equal to the set

$$\Omega_0^d = \{(z, \theta, \tilde{\eta}, \alpha, \beta) : \tilde{d}_i = 0,\ |L_i x \cos\theta_i + L_i y \sin\theta_i| \le \varepsilon, \forall i \in \mathcal{V}\}.$$

Now, applying the hybrid invariance principle, the system converges to the largest weakly invariant set Ω_0^d. □

Note that the convergence to this set is not finite time, because $\tilde{d}$ converges asymptotically to zero and it affects the dynamics of z. For the system (35), expressed in xy-coordinate and affected by the disturbance, the following can be proved.

Corollary 2
All maximal solutions to the hybrid system (35) are bounded.

The proof of the earlier follows a similar trend as the proof of Corollary 1. Now, we present the main result of this section.

Proposition 5
Assume that $\Phi_i^d = -\Phi_i^{d\,T}$, $E_i^d = \Gamma_i^{d\,T}$. Then, all maximal solutions to the hybrid system (35) converges to the following invariant set

$$\left\{(x, y, \theta, \tilde{\eta}, \alpha, \beta) :\ |L_i x| \le \varepsilon,\ |L_i y| \le \delta,\ \theta_i = 0,\ \tilde{d}_i = 0,\ (\alpha_i, \beta_i) = (0, -1)\ \ \forall i \in \mathcal{V}\right\},$$

with $u_i = -\text{sign}_\varepsilon(r_i)$ and $\breve{u}_i = r_i + \text{sign}_\varepsilon(r_i) + \dot{x}_i \cos\theta_i + \dot{y}_i \sin\theta_i$, with $r_i = L_i x \cos\theta_i + L_i y \sin\theta_i$.

Proof
Because $\dot{\theta}_i$ obeys the same dynamic as in the previous section and the sets C^d and D^d do not depend on $\tilde{\eta}$, we can follow the proof of Proposition 3 and Lemma 1. Hence, $|L_i x \cos\theta_i + L_i y \sin\theta_i| \le \varepsilon$ implies that $|L_i x| \le \varepsilon$, $|L_i y| \le \delta$ and $\theta_i = 0$. Moreover, from Proposition 4, $\tilde{\eta}_i$ is bounded. □

DOI: 10.1002/rnc

Notice Proposition 4 states the boundedness of $\tilde{\eta}_i$. The latter also holds for the result of Proposition 5. Continuing with Proposition 5, if we assume $\Phi_i^d = \mathbf{0}$, then $\dot{\tilde{\eta}}_i = {\Gamma_i^d}^T \breve{u}_i$ and $\tilde{d}_i = \Gamma_i^d \tilde{\eta}_i = 0$ hold on the invariant set. Hence, $\breve{u}_i = 0$ and $|L_i x| = 0$. A similar argument holds for the case where ϕ_i^d is a combination of constant and harmonic disturbances (see Figure 9 in Section 6).

6. SIMULATION RESULTS

This section presents the simulation results for a network of four unicycles with the dynamics in (4). The agents are communicating over an undirected and connected graph with the associated Laplacian matrix $L = (L_1^T \dots L_4^T)^T$ with $L_1 = (+1 \ -1 \ 0 \ 0)$, $L_2 = (-1 \ +3 \ -1 \ -1)$, $L_3 = (0 \ -1 \ +2 \ -1)$, $L_4 = (0 \ -1 \ -1 \ +2)$. The initial position of the agents is $q(0,0) = (x(0,0), y(0,0))^T$, where $x(0,0) = (0, 0.1, -0.5, 1.3)$ is the initial position in x-direction and $y(0,0) = (0, -0.4, -1.4, 0.9)$ is the initial position in y-direction. The initial orientation is set to $\theta(0,0) = (0, \pi, -\frac{\pi}{2}, \frac{\pi}{8})$. Moreover, the values for ε, γ, and δ are set to 0.1, 0.2, and 0.3, respectively.

Figure 5 shows the evolution of the average positions and positions of four agents in x and y directions. As shown, each of the four components of the average position in x-direction, Lx, takes a value in the interval $[-0.1, +0.1]$, and each of the four components of Ly takes a value in the interval $[-0.3, +0.3]$.

Figure 6 shows the orientations of the four agents together with the control action u where $u_i = -\text{sign}_\varepsilon(L_i x \cos\theta_i + L_i y \sin\theta_i)$. The orientation of each of the agents converges to zero. Comparing the convergence of Lx (Ly) with θ, it can be seen that Lx (Ly) converges in finite time. The plot of u confirms that the control action u shows a steady chatter-free behavior (see 'Discussion on the control action' after Proposition 3).

However, the control action $u(t)$ for some initial conditions may show transient fast switching before the consensus is reached ([32]). Figure 7 shows the control action of agent 1 with different initial conditions on the positions as $x(0,0) = (0.5, 0.1, -0.5, 1.3)$ and $y(0,0) = (-0.5, -0.4, -1.4, 0.9)$. Potential future solutions for this effect includes improving the ternary controller, for example, to a hybrid sign.

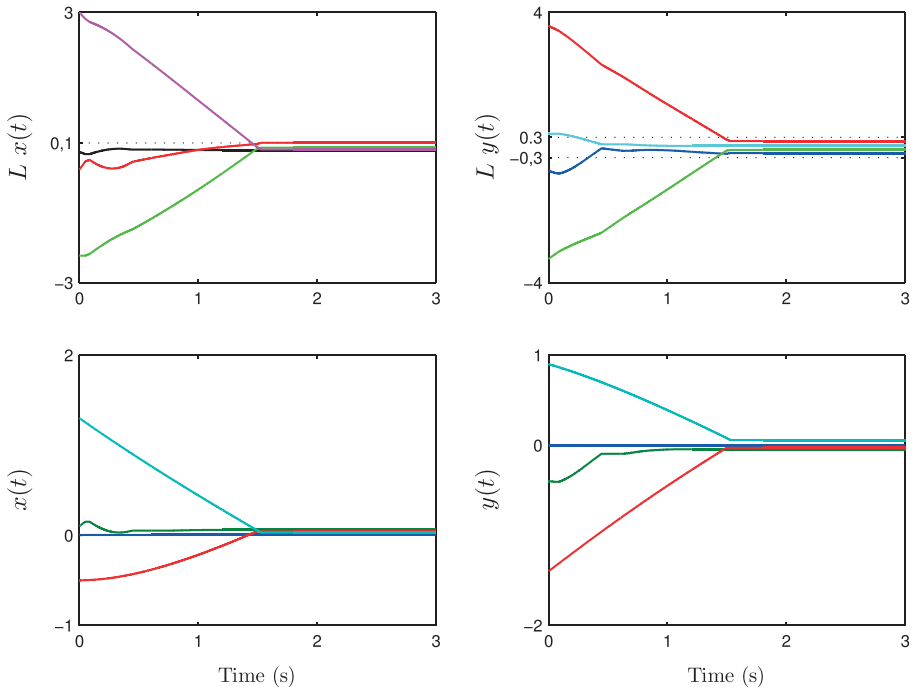

Figure 5. The time evolution of the average positions and positions in x and y directions. [Colour figure can be viewed at wileyonlinelibrary.com]

DOI: 10.1002/rnc

Figure 8 shows the convergence result for a setting, where ε, γ, and δ take different values for different agents (Remark 2). In this example, $\varepsilon_1 = 0.1$, $\gamma_1 = 0.2$, and $\delta_1 = 0.3$; $\varepsilon_2 = 0.3$, $\gamma_2 = 0.4$, and $\delta_2 = 0.5$; and $\varepsilon_3 = \varepsilon_4 = 0.5$, $\gamma_3 = \gamma_4 = 0.6$, and $\delta_3 = \delta_4 = 0.7$. As shown, consensus of the average positions is achieved where the consensus bounds for Lx and Ly are 0.3 and 0.6, respectively. The orientations also converge to zero as in Figure 6.

The results of disturbance rejection (Section 5) are shown in Figure 9. In this simulation, the following are set as the internal model parameters: $\Phi_i^d = \begin{pmatrix} 0 & 0 & 0 \\ 0 & 0 & i+2 \\ 0 & -(i+2) & 0 \end{pmatrix}$, $\Gamma_i^d = (1, 1, 0)$,

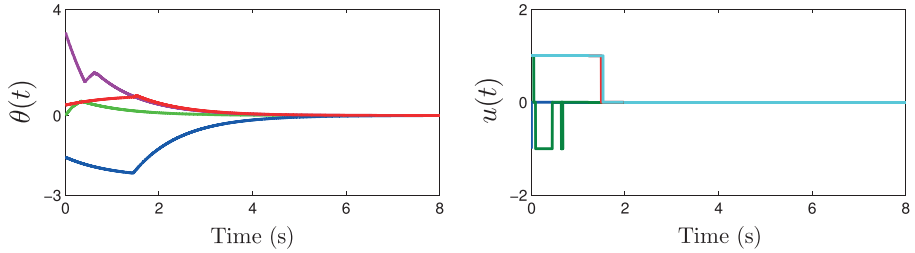

Figure 6. The time evolution of θ together with the control action u. [Colour figure can be viewed at wileyonlinelibrary.com]

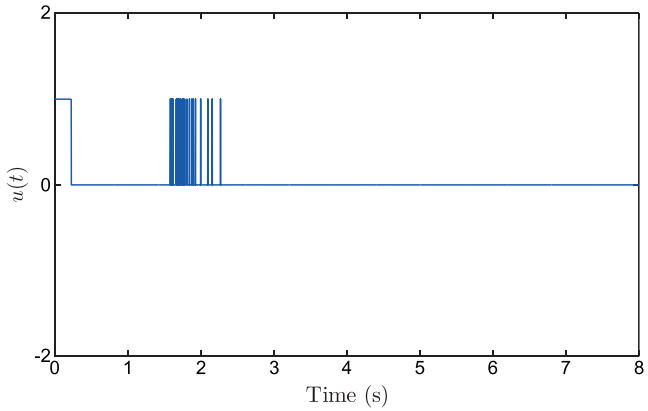

Figure 7. The control action may show transient oscillations depending on initial conditions. [Colour figure can be viewed at wileyonlinelibrary.com]

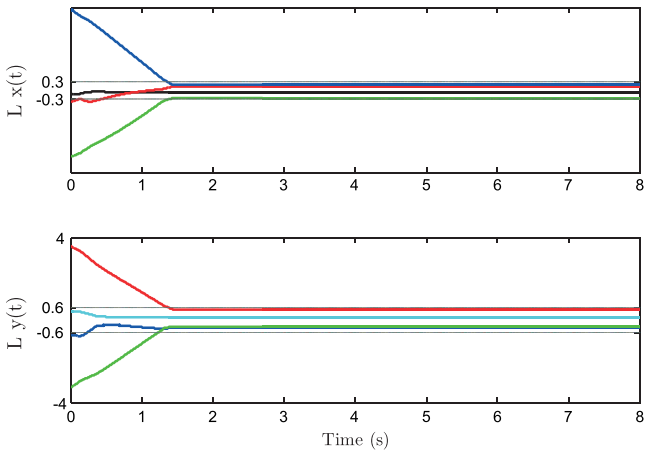

Figure 8. Convergence of average positions of agents with different ε, γ, and δ. [Colour figure can be viewed at wileyonlinelibrary.com]

DOI: 10.1002/rnc

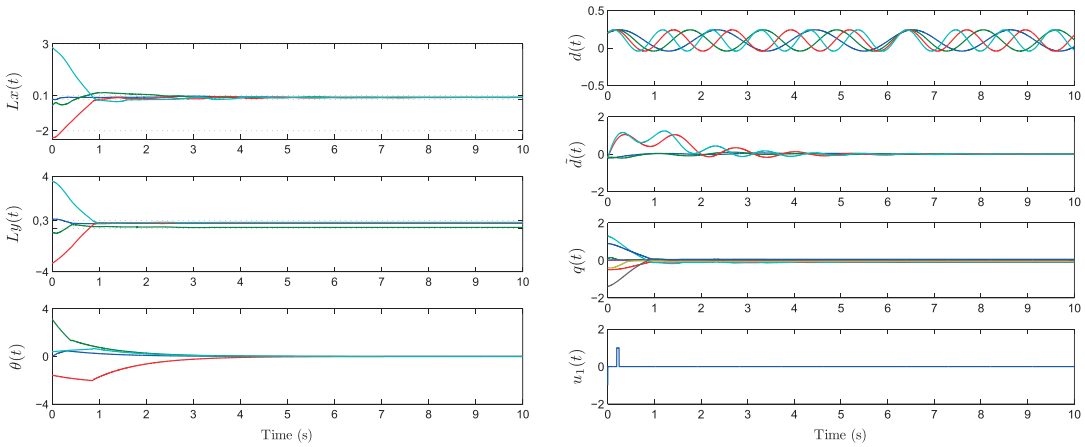

Figure 9. Simulation result of Section 5. [Colour figure can be viewed at wileyonlinelibrary.com]

$G_i^d = \Gamma_i^{d\,T}$, $w_i^d(0) = (0.1, 0.1, 0.1)^T$, and $\eta_i^d(0) = (0, 0, 0)^T$. Also, $\varepsilon = 0.1, \gamma = 0.2, \delta = 0.3$ are set for all agents. As shown, each of the four components of the average position in x-direction, $Lx(t)$, converges to zero, and each of the four components of $Ly(t)$ takes a value in the interval $[-0.3, +0.3]$. Figure 9 shows the disturbance $d(t)$, the disturbance error $\tilde{d}(t)$, the position $q(t)$, the orientation $\theta(t)$ for all of the four agents, and the control signal for agent one $u_1(t)$. As shown, the error disturbance converges to zero, and the position of each agent is bounded. Moreover, the orientation of each of the agents converges to zero.

7. CONCLUSIONS

This paper has presented a robust design for the consensus of unicycles using ternary and hybrid controllers over a connected and undirected graph. The application of ternary controllers has led to a finite-time practical consensus of the agents' average positions. In addition, a hybrid-quantizer-based controller based on an application of the atan2 function has been introduced to steer the orientations of all of the agents to a common value. Furthermore, matched input disturbance rejection for the unicycles of the network has been tackled using an internal-model-based controller. In this case, the convergence of the network has been asymptotic. The analytical results of this paper have been performed in a hybrid framework. Future avenues of the research include relaxing the assumption of a common sense of orientation, improving the design of the ternary controller in order to tackle possible transient oscillations, and considering directed graphs and time-varying communication topologies.

ACKNOWLEDGEMENTS

This research was performed at the University of Groningen (The Netherlands) within the project *Quantized Information Control for Formation Keeping* (QUICK) supported by the Dutch Organization for Scientific Research (NWO). The author would like to thank Claudio De Persis and Jacquelien M.A. Scherpen for their helpful suggestions and constructive comments.

REFERENCES

1. Jadbabaie A, Lin J, Morse AS. Coordination of groups of mobile autonomous agents using nearest neighbor rules. *IEEE Transactions on Automatic Control* 2003; **48**(6):988–1001.
2. Bullo F, Cortés J, Martınez S. *Distributed Control of Robotic Networks*, Applied Mathematics Series. Princeton University Press, 2009.
3. Mesbahi M, Egerstedt M. *Graph Theoretic Methods in Multiagent networks*. Princeton University Press, 2010.
4. Ren W, Beard R. *Distributed Consensus in Multi-vehicle Cooperative Control: Theory and Applications*, Communications and Control Engineering. Springer-Verlag: London, 2008.

DOI: 10.1002/rnc

5. Tanner HG, Jadbabaie A, Pappas GJ. Stable flocking of mobile agents, part I: fixed topology. *42nd IEEE Conference on Decision and Control*, Vol. 2, 2003; 2010–2015.
6. Brockett RW. *Asymptotic Stability and Feedback Stabilization*. Birkhäuser: Boston, 1983.
7. Dimarogonas DV, Kyriakopoulos KJ. On the rendezvous problem for multiple nonholonomic agents. *IEEE Transactions on Automatic Control* 2007; **52**(5):916–922.
8. Lin Z, Francis B, Maggiore M. Necessary and sufficient graphical conditions for formation control of unicycles. *IEEE Transactions on Automatic Control* 2005; **50**(1):121–127.
9. Sadowska A, Kostic D, van de Wouw N, Huijberts H, Nijmeijer H. Distributed formation control of unicycle robots. *IEEE International Conference on Robotics and Automation (ICRA)*, 2012; 1564–1569.
10. Tanner HG, Jadbabaie A, Pappas GJ. *Flocking in teams of nonholonomic agents*, Cooperative Control. Springer: Berlin Heidelberg, 2005: 229–239.
11. Zheng R, Lin Z, Cao M. Rendezvous of unicycles with continuous and time-invariant local feedback. *Proceedings of the 18th IFAC World Congress*, Vol. 18, 2011; 10044–10049.
12. Oikonomopoulos AS, Loizou SG, Kyriakopoulos KJ. Hybrid control of a constrained velocity unicycle with local sensing. *Decision and Control, 2008. CDC 2008. 47th IEEE Conference on*: IEEE, 2008; 1753–1758.
13. Kwok A, Martìnez S. Unicycle coverage control via hybrid modeling. *IEEE Transactions on Automatic Control* 2010; **55**(2):528–532.
14. Chen G, Lewis FL, Xie L. Finite-time distributed consensus via binary control protocols. *Automatica* 2011; **47**(9):1962–1968.
15. Cortés J. Finite-time convergent gradient flows with applications to network consensus. *Automatica* 2006; **42**(11):1993–2000.
16. Jafarian M, Vos E, De Persis C, Scherpen JMA, van der Schaft AJ. Formation control of a multi-agent system subject to Coulomb friction. *Automatica* 2015; **61**:253–262.
17. Jafarian M, De Persis C. Formation control using binary information. *Automatica* 2015; **53**:125–135.
18. Yu J, LaValle SM, Liberzon D. Rendezvous without coordinates. *IEEE Transactions on Automatic Control* 2012; **57**(2):421–434.
19. Isidori A, Marconi L, Serrani A. *Robust Autonomous Guidance: An Internal Model Approach*. Springer: London, U.K., 2003.
20. De Persis C, Jayawardhana B. On the internal model principle in the coordination of nonlinear systems. *IEEE Transactions on Control of Network Systems* 2014; **1**(3):272–282.
21. Jafarian M, Vos E, De Persis C, Scherpen JMA, van der Schaft AJ. Disturbance rejectionin in formation keeping control of nonholonomic wheeled robots. *International Journal of Robust and Nonlinear Control* 2016; **26**:3344–3362. DOI: 10.1002/rnc.3510.
22. Ceragioli F, De Persis C, Frasca P. Discontinuities and hysteresis in quantized average consensus. *Automatica* 2011; **47**(9):1916–1928.
23. Jafarian M. Ternary and hybrid controllers for the rendezvous of unicycles. *Decision and Control (CDC), 2015 IEEE 54th Annual Conference on*: IEEE, 2015; 2353–2358.
24. Bacciotti A, Ceragioli F. Stability and stabilization of discontinuous systems and nonsmooth Lyapunov functions. *ESAIM: Control, Optimisation and Calculus of Variations* 1999; **4**:361–376.
25. Goebel R, Sanfelice RG, Teel AR. *Hybrid Dynamical Systems: Modeling, Stability, and Robustness*. Princeton University Press, 2012.
26. Danca MF. Synchronization of piece-wise continuous systems of fractional order. *arXiv preprint arXiv:1402.6986* 2014.
27. Paden B, Sastry S. A calculus for computing Filippov's differential inclusion with application to the variable structure control of robot manipulators. *IEEE Transactions on Circuits and Systems* 1987; **34**(1):73–82.
28. De Persis C, Postoyan R. A Lyapunov redesign of coordination algorithms for cyberphysical systems. *IEEE Transactions on Automatic Control* 2017; **62**:808–823.
29. Sanfelice RG, Biemond JJ, van de Wouw N, Heemels WP. An embedding approach for the design of state-feedback tracking controllers for references with jumps. *International Journal of Robust and Nonlinear Control* 2014; **24**(11):1585–1608.
30. Cortés J, Bullo F. Coordination and geometric optimization via distributed dynamical systems. *SIAM Journal on Control and Optimization* 2005; **44**(5):1543–1574.
31. Jafarian M, De Persis C. Exact formation control with very coarse information. *American Control Conference (ACC)*, 2013; 3026–3031.
32. Jafarian M. A note on formation keeping control with coarse information. *International Symposium on Mathematical Theory of Networks and Systems*, 2014; 1724–1727.